**Supporting Information**

# Wooden electrothermal composites for fast electrothermal conversion

Yuting Zhang, Hengsong Zheng, Sijia Sun, Shuaiqi Wang, Mingzhu Pan*

College of Materials Science and Engineering, Co-Innovation Centre of Efficient Processing and Utilization of Forest Resources, Nanjing Forestry University, Nanjing 210037, China

* *Correspondence to*: *Dr.* M.Z. Pan (mzpan@njfu.edu.cn); tel: (86-25)-8542 8518

***2.1 Materials***

*Balsa* (ρ= 0.16g /cm$^3$, 50×30 mm) was purchased from online store. Chitosan (CS, viscosity: 50-800 MPa·s, degree of deacetylation: 80.0%-95.0%) was provided by Sinopharm Chemical Reagent Co., Ltd. (Shanghai, China). Phytic acid (PA, $C_6H_{18}O_{24}P_6$) was purchased by shanghai Maclean biochemical technology co., Ltd. (Shanghai, China). MAX and Lithium fluoride (LiF) was purchased from Shanghai Aladdin Biochemical Technology Co., Ltd. (Shanghai, China). $NaClO_2$ was provided by Sinopharm Chemical Reagent Co., Ltd. (Shanghai, China). Acetic acid ($CH_3COOH$, ≥ 99.5 wt%), hydrochloric acid (HCl) and anhydrous ethanol (≥99.7 wt%) were purchased from Nanjing Chemical Reagent Co., Ltd. (Nanjing, China). Anhydrous potassium carbonate ($K_2CO_3$ ≥99.0 wt%) was obtained from Lingfeng Chemical Reagent Co., Ltd. (Shanghai, China). Sodium chloride (NaCl ≥ 99.5 wt%) were purchased from Chemical Reagent Co., Ltd. (Nanjing, China). All chemicals are chemically pure and were used without further purification.

***2.2 Preparation of MXene***

The relationship between MXene loading and conductivity corresponding to different MXene concentration gradients are as shown in Table S1.

**Table S1.** Relationship between MXene loading and conductivity corresponding to different MXene concentration gradients.

| MXene concentration (mg/mL) | MXene loading (g/m$^2$) | Electrical conductivity (S/m) |
|---|---|---|
| 15 | 10.0 | 145.4<br>(7.23) |
| 20 | 13.3 | 175.5<br>(9.11) |
| 25 | 16.7 | 214.4<br>(7.25) |
| 30 | 20.0 | 251.7<br>(7.49) |
| 35 | 23.3 | 239.8<br>(9.62) |

Notes: (*x*) means the standard deviation of the data.

### *2.4 Characterizations*

***Morphology and structure*:** The microstructures and morphologies of MXene nanosheet was observed by TEM (JEM-2100, Nihon Electronics Co., Japan) and XRD (Ultrima Type IV, Rigaku, Japan). The ultrastructure of as-prepared wooden electrothermal composites were analyzed by FTIR (a VERTEX 80 IR, Bruker, Germany), XPS (AXIS UltraDLD, Shimadzu, UK). The morphology and elements distribution of wooden electrothermal composites were performed with a FE-SEM (QUANTA 200, FEI, USA) and energy-dispersive X-ray spectrometer (EDS, Aztec X-Max 80, Oxford, UK). The thermal stability was evaluated with a NETZSCH TG 209 F3.

***Mechanical property*:** The tensile strength properties were evaluated by microcomputer-controlled electronic universal mechanical testing machine (CMT6104 type, Shenzhen New Sansi Materials Testing Co., Ltd.).

***Flame retardancy:*** Flame retardancy was measured by cone calorimeter (CC, Fire Testing Technology, UK) according to ISO 5660-2002 at a heat flux of 50 $kW/m^2$, limiting oxygen index (LOI) values according to ISO 4589, respectively.

***Electrothermal stability:*** The humidity in the chamber was regulated by saturated $K_2CO_3$ and NaCl solutions at 44 %, 76 %, and 99 % relative humidity (RH). A calibrated traceable digital hygrometer (HTC-1, Apuhua, China) was used to monitor the RH inside the desiccator. The environment temperature was controlled by refrigerator and oven temperatures of -18 °C, 25 °C and 40 °C, respectively. The voltage is applied via a direct voltage (DC) power source (MS-3010DS, Maisheng). The temperature changes were monitored using an infrared thermometer (FLIR C5, FLIR Systems Inc.).

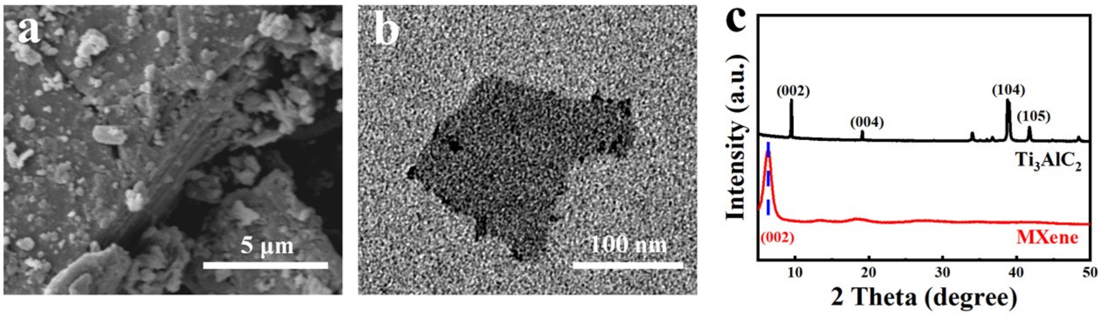


**Fig. S1.** TEM photos of (a) $Ti_3AlC_2$ MAX and (b) single-layered MXene nanosheet, (c) XRD patterns of $Ti_3AlC_2$ MAX and MXene.

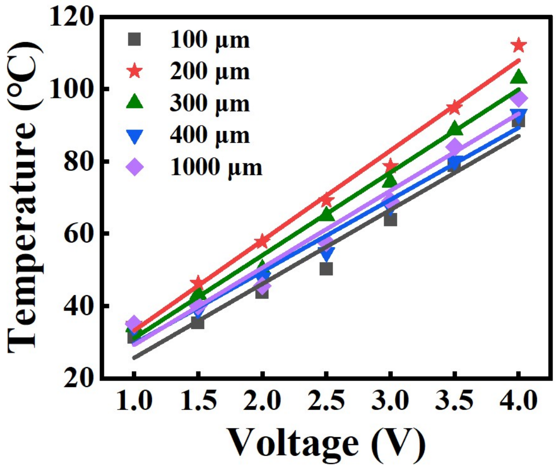


**Fig. S2.** Voltage-temperature curves of electrothermal composites with different thicknesses of wood film.

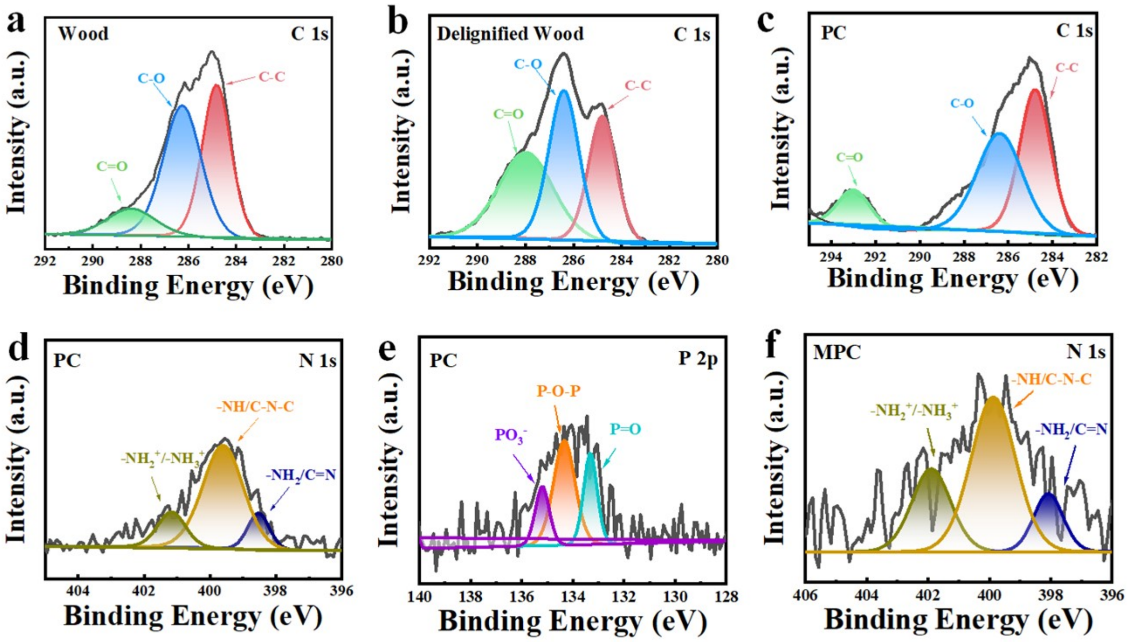


**Fig. S3.** High-resolution XPS spectra of wood C 1 (a), delignified wood C 1s (b), PC C 1s (c), PC N 1s (d), PC P 2p (e) and MPC N 1s (f).

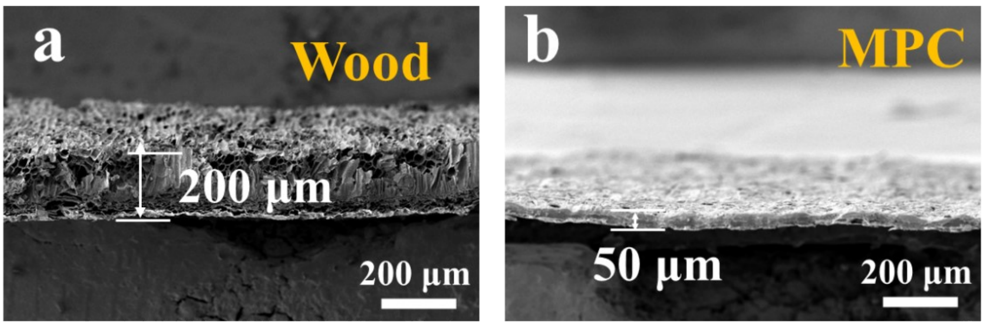


**Fig. S4.** SEM of cross-section (a) natural balsa wood film and (b) the MPC.

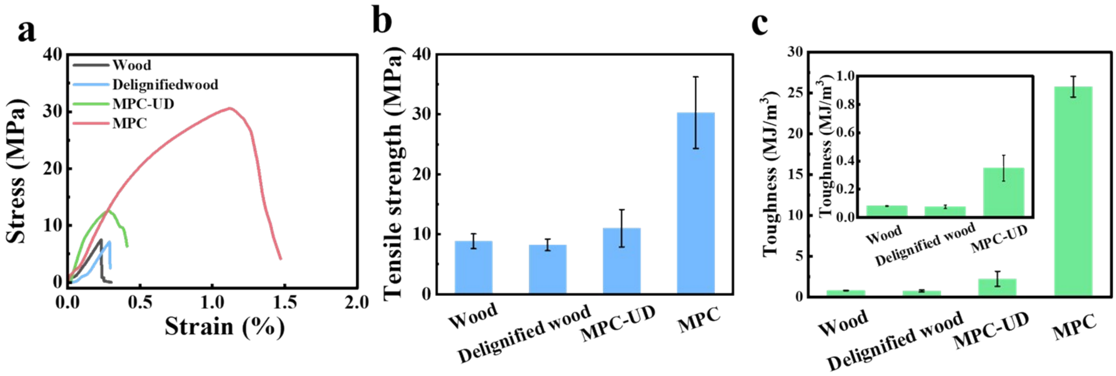


**Fig. S5.** The mechanical properties of wood, delignified wood, MPC-UD and MPC. (a) Stress-strain curves, (b) Tensile strength, (c) Toughness.

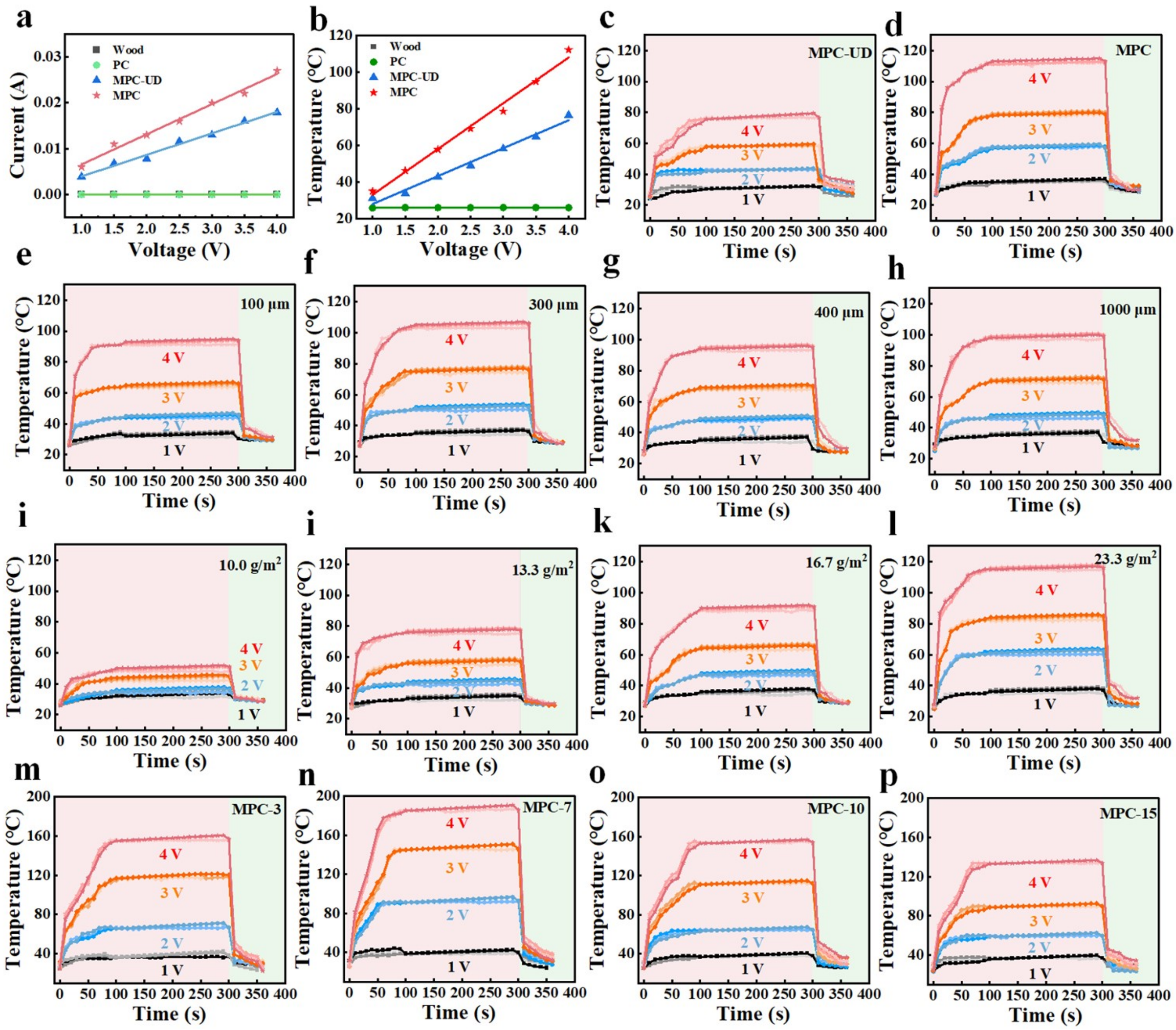


**Fig. S6.** (a) Voltage-current linear curves and (b) Voltage-temperature curves of wood, PC, MPC-UD and MPC , (c) Time-temperature curves at different applied voltages of MPC-UD, (d) Time-temperature curves at different applied voltages of MPC, (e-h) Time-temperature curves at different applied voltages of MPC with different thickness, (i-l) Time-temperature curves at different applied voltages of MPC with different MXene content, (m-p) Time-temperature curves at different applied voltages of MPC-*n* (*n*=3, 5, 7, 10, 15).

**Table S2.** The saturation temperature of MPC-*n* (*n*=1, 3, 5, 7, 10, 15) from 1~4 V.

| Category | Saturation temperature (°C) | | | |
|---|---|---|---|---|
| | 1 V | 2 V | 3 V | 4 V |
| MPC | 35.47 (0.57) | 58.0 (0.65) | 79.0 (1.10) | 112.73 (1.18) |
| MPC-3 | 38.43 (1.45) | 67.83 (1.33) | 119.33 (1.16) | 157.50 (1.22) |
| MPC-5 | 41.13 (1.16) | 86.93 (1.76) | 137.40 (1.23) | 181.90 (1.65) |
| MPC-7 | 39.70 (1.44) | 93.46 (1.18) | 147.43 (1.24) | 187.1 (1.82) |
| MPC-10 | 38.50 (0.69) | 65.23 (0.63) | 112.80 (0.61) | 154.97 (0.32) |
| MPC-15 | 37.60 (0.52) | 60.37 (0.75) | 90.53 (0.46) | 135.00 (0.26) |

Notes: (*x*) means the standard deviation of the data.

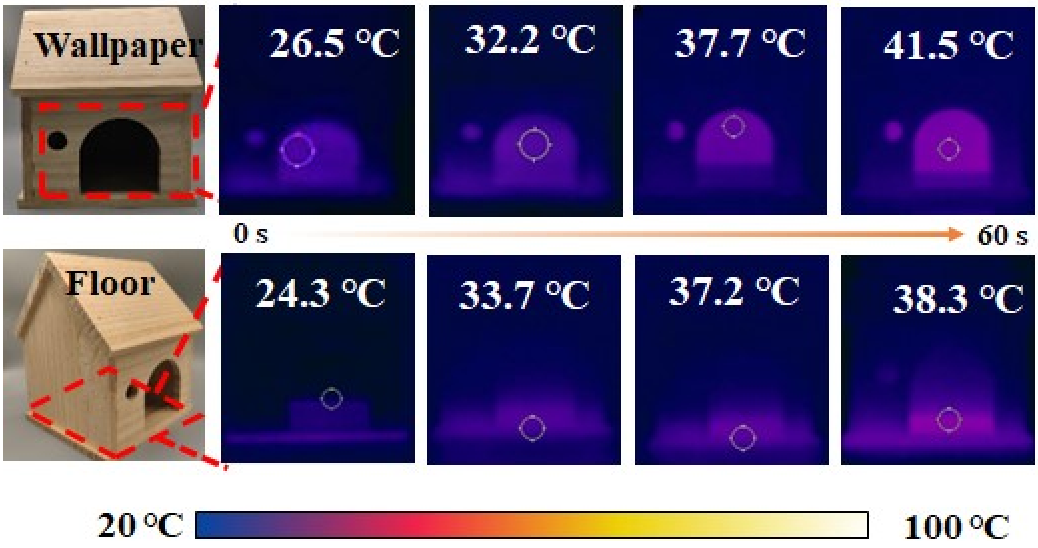


**Fig. S7.** Photographs and thermal images of the warming process of MPC-5 for practical applications as wallpaper and flooring.

**Table S3.** Comparison between the electrothermal performance measured in this study and other electrothermal composites.

| Number | Material | Voltage (V) | Temperature (°C) | Electrothermal conversion efficiency (%) | References |
|---|---|---|---|---|---|
| 1 | CNF/MXene-TA | 12.5 | 90 | 48.5 | 1 |
| 2 | MXene/DW film | 6.0 | 162 | 57.8 | 2 |
| 3 | MMW | 4.0 | 119.3 | 49.7 | 3 |
| 4 | PMP-60 | 3 | 114.9 | 51.3 | 4 |
| 5 | Ni@NCNT-2 | 3.0 | 146.5 | 51.4 | 5 |
| 6 | CWF/EP/Co | 5.0 | 110.2 | 60.7 | 6 |
| 7 | CWF/ZIF-8 | 5.0 | 100 | 53.1 | 7 |
| 8 | Silicone–MXene/CNF | 10.0 | 100 | 62.0 | 8 |
| 9 | Carbonized wood | 2.5 | 100 | 42.2 | 9 |
| 10 | MXene/BF | 2.5 | 49 | 42.7 | 10 |
| 11 | BC/PM | 6.0 | 85 | 54 | 11 |
| 12 | MPC-5 | 4.0 | 180 | 66.7 | This work |

**Table.S4.** Simulation parameters and boundary conditions.

| Size of single filament | Length (mm) | Width (mm) | Height (mm) |
|---|---|---|---|
| | 50 | 30 | 0.2 |
| Thermal conductivity (TC) | 0.463 $Wm^{-1}K^{-1}$ | | |
| Convection coefficient (h) | 8 $Wm^{2}K^{-1}$ | | |
| Specific heat capacity (Cp) | 2400 J $kg^{-1}$ $K^{-1}$ | | |
| Density (ρ) | 116 kg $m^{-3}$ | | |
| Initial temperature | 293.15 K | | |

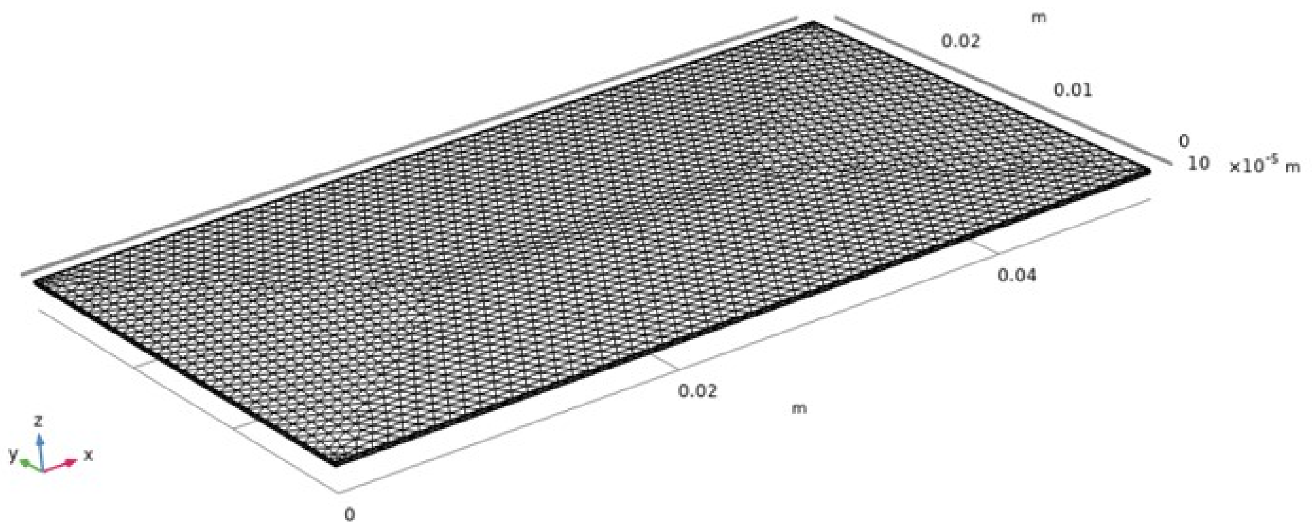


**Fig. S8.** Mesh generation for MPC-5 structure.

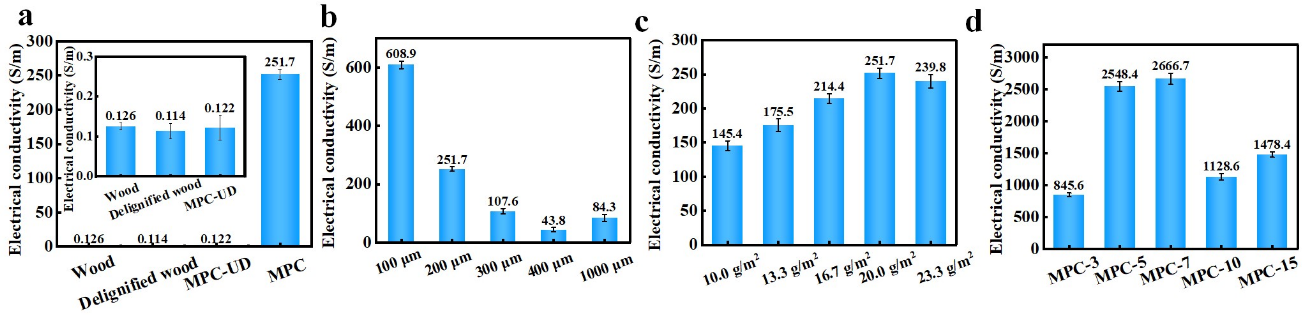


**Fig. S9.** Electrical conductivity of (a) wood, PC, MPC-UD and MPC, (b) MPC with different thickness, (c) MPC with different MXene content,(d) MPC-*n* with diferent layer.

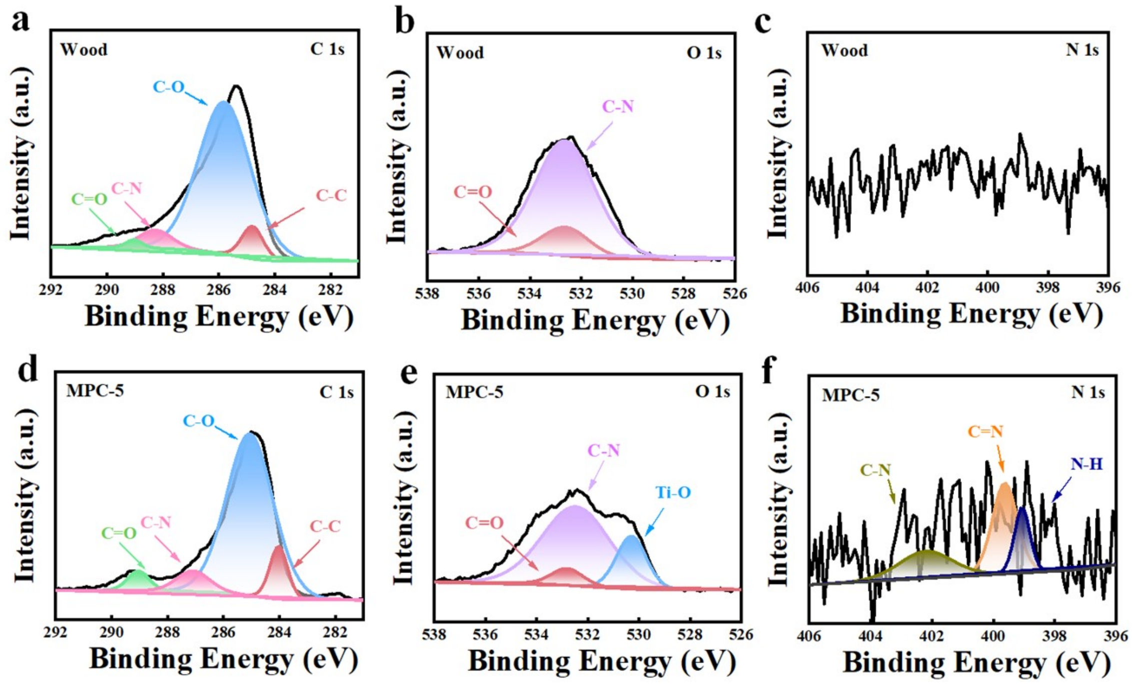


**Fig. S10.** High-resolution XPS spectra of wood C 1s (a), O 1s (b), N 1s (c), and MPC-5 C 1s (d), O 1s (e), N 1s (f).

**Reference:**


1. J. Wei, S. Jia, J. Wei, C. Ma and Z. Shao, Tough and Multifunctional Composite Film Actuators Based on Cellulose Nanofibers toward Smart Wearables, *ACS Appl. Mater. Interfaces*, 2021, **13**, 38700-38711.
2. J. Zhang, L. zhang, C. Lv, L. Gao, X. Chen, S. Luo, Y. Chen, Y. Ren, L. Chang, W. Guo and Q. Tang, Lightweight, ultra-strength, multifunctional MXene/wood composite film designed by densification strategy for electrode, thermal management, and electromagnetic shielding application, *Ind. Crops Prod.*, 2024, **216**, 118700.
3. X. Tao, D. Tian, S. Liang, P. Jiang and F. Fu, Construction of multifunctional surface to fabricate wood-derived cellulose electrothermal composites with flame retardant and hydrophobic performance for harsh operating conditions, *Ind. Crops Prod.*, 2023, **202**, 117079.
4. S. Gong, X. Sheng, X. Li, M. Sheng, H. Wu, X. Lu and J. Qu, A Multifunctional Flexible Composite Film with Excellent Multi-Source Driven Thermal Management, Electromagnetic Interference Shielding, and Fire Safety Performance, Inspired by a "Brick–Mortar" Sandwich Structure, *Adv. Funct. Mater.*, 2022, **32**, 2200570.
5. X. Hao, D. Li, X. Peng, W. Lan and C. Liu, In situ construction of biomass derived 3D carbon framework for efficient electromagnetic interference shielding and Joule heating performance, *Chem. Eng. J.*, 2024, **479**, 147681.
6. X. Ma, S. Liu, H. Luo, H. Guo, S. Jiang, G. Duan, G. Zhang, J. Han, S. He, W. Lu and K. Zhang, MOF@wood Derived Ultrathin Carbon Composite Film for Electromagnetic Interference Shielding with Effective Absorption and Electrothermal Management, *Adv. Funct. Mater.*, 2024, **34**, 2310126.
7. X. Ma, J. Pan, H. Guo, J. Wang, C. Zhang, J. Han, Z. Lou, C. Ma, S. Jiang and K. Zhang, Ultrathin Wood-Derived Conductive Carbon Composite Film for Electromagnetic Shielding and Electric Heating Management, *Adv. Funct. Mater.*, 2023, **33**, 2213431.
8. W. Xin, M.-G. Ma and F. Chen, Silicone-Coated MXene/Cellulose Nanofiber Aerogel Films with Photothermal and Joule Heating Performances for Electromagnetic Interference Shielding, *ACS Appl. Nano Mater.*, 2021, **4**, 7234-7243.
9. B. Zhao, P. Bai, S. Wang, H. Ji, B. Fan, R. Zhang and R. Che, High-Performance Joule Heating and Electromagnetic Shielding Properties of Anisotropic Carbon Scaffolds, *ACS Appl. Mater. Interfaces*, 2021, **13**, 29101-29112.
10. W.-B. Zhu, F.-L. Yi, P. Huang, H. Zhang, Z.-H. Tang, Y.-Q. Fu, Y.-Y. Wang, J. Huang, G.-H. Dong, Y.-Q. Li and S.-Y. Fu, Flexible but robust $Ti_3C_2T_x$ MXene/bamboo

microfibril composite paper for high-performance wearable electronics, Journal of Materials Chemistry A, 2021, 9, 26758-26766.

11. T. Zhang, B. Song, J. Yang, B. Yuan and J. Ma, Vacuum-assisted multi-layer bacterial cellulose/polydopamine-modified MXene film for joule heating, photo thermal, and humidity sensing, *Cellulose*, 2023, **30**, 4373-4385.